Deep-Sea Research I 116 (2016) 14–21

Contents lists available at ScienceDirect

Deep-Sea Research I

journal homepage: www.elsevier.com/locate/dsri

Incrementing data quality of multi-frequency echograms using the Adaptive Wiener Filter (AWF) denoising algorithm

M. Peña

Instituto Español de Oceanografía, Centro oceanográfico de Baleares, Palma de Mallorca, Spain

ARTICLE INFO

Article history:
Received 21 January 2016
Received in revised form
2 June 2016
Accepted 19 July 2016
Available online 27 July 2016

Keywords:
Echogram noise
AWF denoising
TVG
Local variance

ABSTRACT

Achieving acceptable signal-to-noise ratio (SNR) can be difficult when working in sparsely populated waters and/or when species have low scattering such as fluid filled animals. The increasing use of higher frequencies and the study of deeper depths in fisheries acoustics, as well as the use of commercial vessels, is raising the need to employ good denoising algorithms. The use of a lower Sv threshold to remove noise or unwanted targets is not suitable in many cases and increases the relative background noise component in the echogram, demanding more effectiveness from denoising algorithms. The Adaptive Wiener Filter (AWF) denoising algorithm is presented in this study. The technique is based on the AWF commonly used in digital photography and video enhancement. The algorithm firstly increments the quality of the data with a variance-dependent smoothing, before estimating the noise level as the envelope of the Sv minima. The AWF denoising algorithm outperforms existing algorithms in the presence of gaussian, speckle and salt & pepper noise, although impulse noise needs to be previously removed. Cleaned echograms present homogenous echotraces with outlined edges.

1. Introduction

Acoustic surveys are often employed to study the abundance and distribution of pelagic and semi-pelagic species. An acceptable signal-to-noise ratio (SNR) is needed, which may require improvement through noise recognition and elimination. Echogram denoising for small pelagic fish studies with low frequencies (18, 38 kHz) in shelf areas is often performed with the application of a lower threshold for the volume backscattering (Sv, dB re m^{-1}). However, when working with higher frequencies (70, 120, 200, 333 kHz), deeper areas or lower scatterers such as micronekton or plankton (Peña et al., 2014), the lower threshold has to be decreased. Determination of the correct threshold to reduce the amount of noise has always been a relatively arbitrary operation (Nunnallee, 1990). The main inconvenience of lowering the threshold is the relative increase in the background noise component in the echogram, particularly for high frequencies, which requires treatment via a denoising algorithm. Where there is a target with a low signal to noise ratio it may not be appropriate to correct for background noise by thresholding; the correct approach is to correct for noise.

In fisheries acoustics the term background noise refers to ambient and vessel noise that affects all pings. It can vary in intensity and pattern with vessel speed, engine rpm, propeller pitch and bottom depth etc. Scientific echosounders compensate for range-dependent signal attenuation due to absorption and beam spreading using a time-varied-gain (TVG) function; for volume backscatter, Sv db re 1 m^{-1}, the TVG function is $20^{*}\log R+20^{*}\alpha^{*}R$ with R being range and α the attenuation coefficient. Thus measured Sv values should be range-independent. Background noise on the other hand is ubiquitous and independent of the echosounder's transmit-receive cycle, thus its value will be increased by range according to the TVG function. Further, the absorption component of the TVG function increases with frequency. Thus comparisons across frequencies become biased by the TVG amplified noise as a function of range and frequency. The utility of multifrequency data in terms of range performance can therefore be extended through the application of background noise algorithms.

Denoising algorithms focused in the past on removing background noise. Watkins and Brierley (1996) developed a method to eliminate it, after removing TVG, by estimating the noise as the offset of the least square fitting of the Sv minima curve. Korneliussen (2000) considered noise variation with time by estimating noise as the minimum Sv value of each ping, considering enough below bottom or long range samples, in order to ensure the existence of samples dominated by noise. Finally deRobertis and Higginbottom (2007) considered the high variability in the data and estimated noise from a smoothed version of the echogram in regular bins. This estimated noise was proven equivalent to the background noise detected in passive mode. This background

E-mail address: marian.pena@ba.ieo.es

http://dx.doi.org/10.1016/j.dsr.2016.07.008
0967-0637/

noise is subtracted and the SNR can be calculated and used for further thresholding of the echogram. All the previous techniques remove noise from the echogram, but maintain the data quality unmodified. A gaussian smoothing is previously applied by de-Robertis and Higginbottom (2007) for a better noise estimation, but the signal variability remains very similar.

The natural stochastic fluctuations in acoustic data requires some pre-processing smoothing. However, usual averaging techniques, such as convolution, cause blurring, which affects edge information. The high variability of noise requires adaptive filtering, based on local noise. Korneliussen and Ona (2003) greatly improved the accuracy of the frequency response by smoothing the data first, but they acknowledged the need to apply different smoothing to different areas of the echogram. The aim of this study was to present a new algorithm for denoising echograms that firstly increments data quality with smoothing based on local variance, and then provides a non-arbitrary threshold to remove noise. The algorithm reduces the echogram variability, but maintaining the spatial structures such as school shapes and edges, and incrementing SNR. The TVG amplification of background noise is greatly reduced and more biologically relevant information is kept. The algorithm is compared with the technique introduced by de-Robertis and Higginbottom (2007).

2. Material and methods

The method was applied to four surveys on board three different vessels and in four different areas to check general suitability. Results from the JUVENA 2013 survey on board the RV *Ramón Margalef* are presented. The echograms show a mixture of unsampled shoals recorded in September on the slope of the French shelf in the Bay of Biscay. Acoustic backscattering was recorded with a sphere calibrated (Demer et al., 2015) Simrad EK60 echosounder, using the split-beam transducers to record at multiple frequencies simultaneously (available frequencies: 18, 38, 70, 120, 200, and 333 kHz, but we do not present the 70 and 120 kHz results, as they were less relevant). No volume backscatter (Sv, dB re m^{-1}) threshold was employed in the analysis, but the final echograms are presented from −90 to −50 dB for comparison. All data were processed in Matlab.

2.1. Denoising

The Adaptive Wiener Filter (AWF) is frequently used in digital photography and video (Lim, 1990). In this study the AWF is used within a novel algorithm (hereafter named 'AWF denoising algorithm'), applied to each frequency echogram after TVG subtraction. The AWF algorithm is a low-pass filter that applies pixel-wise adaptive denoising that varies with the variance in the surrounding neighbourhood. The degree of smoothing is inversely proportional to the variance, which increases the edge information while blurring the rest. A 3 × 3 window was selected. If the unclean image has a low signal-to-noise ratio (SNR), some noise can remain in the echogram, because there is a large difference between the estimated and actual noise (see Abe and Shimamura (2012) for more details). To overcome this issue, the algorithm was applied iteratively (ten times) so that the estimated noise approached the real value.

An estimate of the noise value can then be calculated as the envelope (maximum) of Sv minima over a running window of *n* values. The number of pings in the window was set to 60, due to the stability of the results. The noise value was used as a threshold to clean the echogram and then the TVG was added back on. An extra threshold was employed, as done by deRobertis and Higginbottom (2007), removing pixels with SNR lower than 3 dB (the SNR threshold was increased to 5 dB for the 333 kHz echograms). Following deRobertis and Higginbottom (2007) nomenclature, the algorithm used was as follows:

$$
\begin{aligned}
Power(i,j) &= Sv_{meas}(i,j) - 20\log_{10}(z(i,j)) - 2\alpha z(i,j)\mu(i,j) \\
&= \frac{1}{N*M}\sum_{i,j\epsilon\eta} Power(i,j)\sigma^2(i,j) \\
&= Power(i,j)^2 - \mu(i,j)^2 v^2 = \frac{1}{npixels}\sum_{i,j}\sigma^2(i,j) \\
&Sv_{cleaned}(i,j) \\
&= \left[\mu(i,j) + \frac{\sigma^2(i,j) - v^2}{\sigma^2(i,j)}(Power(i,j) - \mu(i,j))\right]_{x10} \\
&Noise(j) = \max(\min(Sv_{cleaned}(i,j))_{\epsilon[j,j+60]}) \\
&Sv_{thresholded}(i,j) = \left[Sv_{cleaned}(i,j)\right]_{>Noise(j)} Sv_{noise}(i,j) \\
&= Noise(i) + 20\log_{10}(z(i,j)) + 2\alpha z(i,j) Sv_{denoised}(i,j) \\
&= Sv_{thresholded}(i,j) + 20log_{10}(z(i,j)) + 2\alpha z(i,j) SNR(i,j) \\
&= Sv_{denoised}(i,j) - Sv_{noise}(i,j) Sv_{thresholded}(i,j) \\
&= \left[Sv_{denoised}(i,j)\right]_{SNR(i,j)>3}
\end{aligned}
\tag{1}
$$

where i and j are sample and ping respectively; Sv_{meas} is the volume backscatter recorded by the echosounder; $z(i,j)$ the depth value, corrected with the pulse duration and sound speed; α the absorption coefficient; $\mu(i,j)$ and $\sigma^2(i,j)$ are the mean and variance in the local neighbourhood (η) of *N* by *M* pixels (3 × 3 in this case); and *npixels* is the number of pixels in the echogram. The term $\frac{\sigma^2(i,j) - v^2}{\sigma^2(i,j)}$ acts as a variance-dependent smoother coefficient: the higher the local variance $\sigma^2(i,j)$ with respect to the total echogram variance v^2, the closer the term is to one, resulting in less smoothing. The *x*10 symbol indicates the 10 times iteration of the AWF denoising employed to reach actual local noise (recalculating $\mu(i,j)$, $\sigma^2(i,j)$ and v^2). The results of the minimum values before and after applying the AWF filter and the employed threshold are shown.

The new AWF denoising algorithm described was compared with the background noise removal implemented by the most commonly employed commercial software, Echoview, as described by deRobertis and Higginbottom (2007). A 3 × 3 gaussian smoothing was previously applied as recommended by the author. This denoising algorithm finds the noise value for each pixel as the minimum *Sv* of the echogram, averaged in an *M* by *N* window (*M*=20 samples and *N*=30 pings). The TVG previously subtracted from the echogram is added to the noise value, and the total subtracted from the original echogram in the linear domain. The SNR threshold of 3 dB (or 5 dB for 333 kHz) is then applied.

2.2. Method comparison

To quantitatively compare both methods, an estimate of the remaining Gaussian noise was measured following Immerkr (1996) with the matlab implementation available in Birdal (2016) that convolves the test image with a reference kernel to quantify noise. This includes a Laplacian operation which is almost insensitive to image structure and only depends on the noise in the image. This value is estimated for the whole echogram, covering almost an hour of recording. A domain covering the most biologically important area in the echograms was defined and marked with a black square. Then, two percentages were calculated within that domain for each echogram: (1) the percentage of impulse noise in that square, calculated as the percentage of pixels exceeding 10 dB from the previous or following ping, or vertical

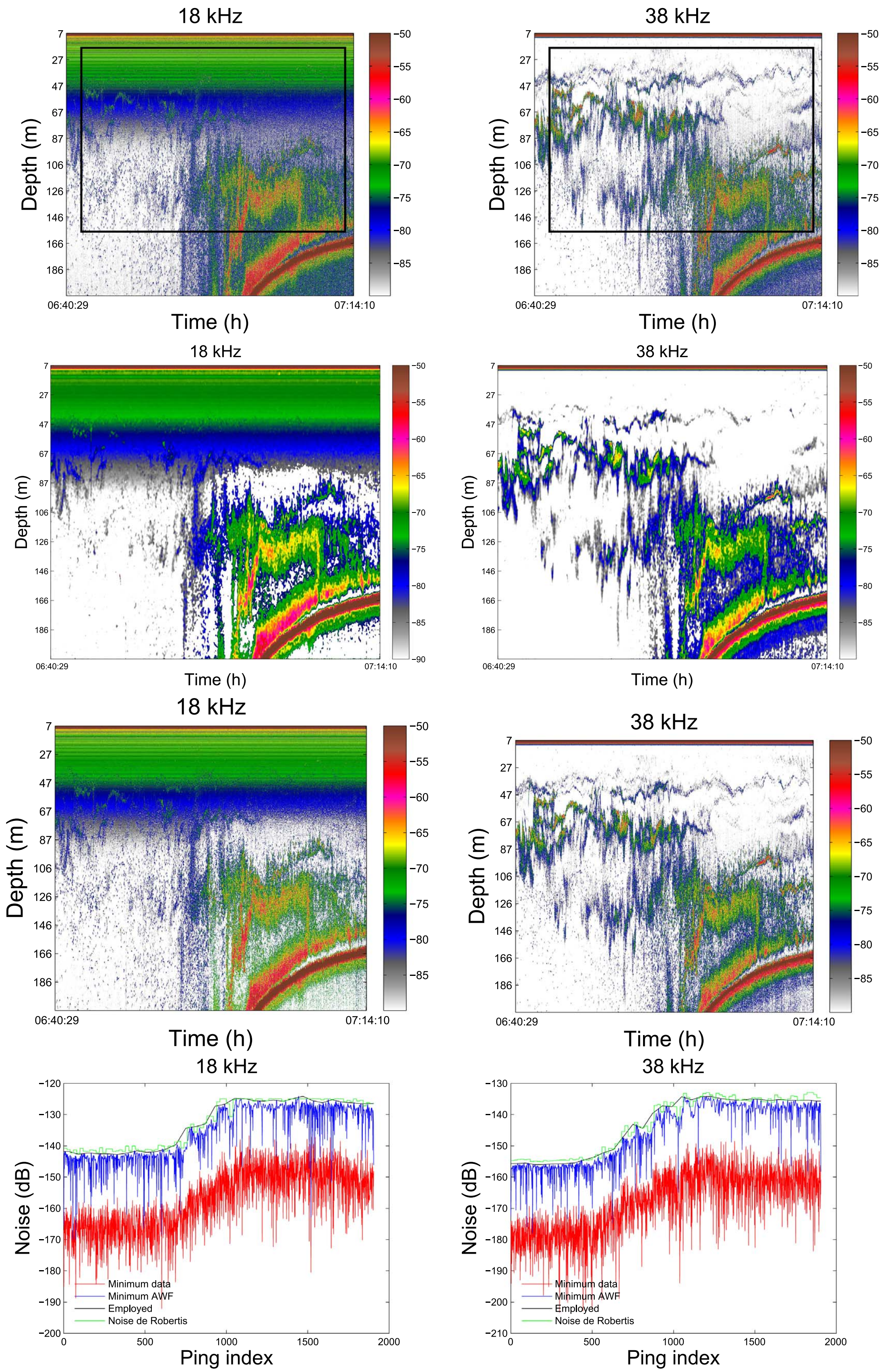

Fig. 1. Denoising of the 18 and 38 kHz showing: (first row) the original, (second row) the AWF denoising algorithm-processed, and (third row) the deRobertis and Higginbottom (2007) algorithm-processed echograms, and (forth row) the minimum *Sv* values before ('minimum Sv') and after applying the AWF denoising ('minimum AWF') without TVG-amplification. The 'employed' level is the envelope of the minimum *Sv* values after smoothing. The noise level estimated by the deRobertis and Higginbottom (2007) method is also included. The square in the original echogram marks the area employed to calculate variables in Table 1.

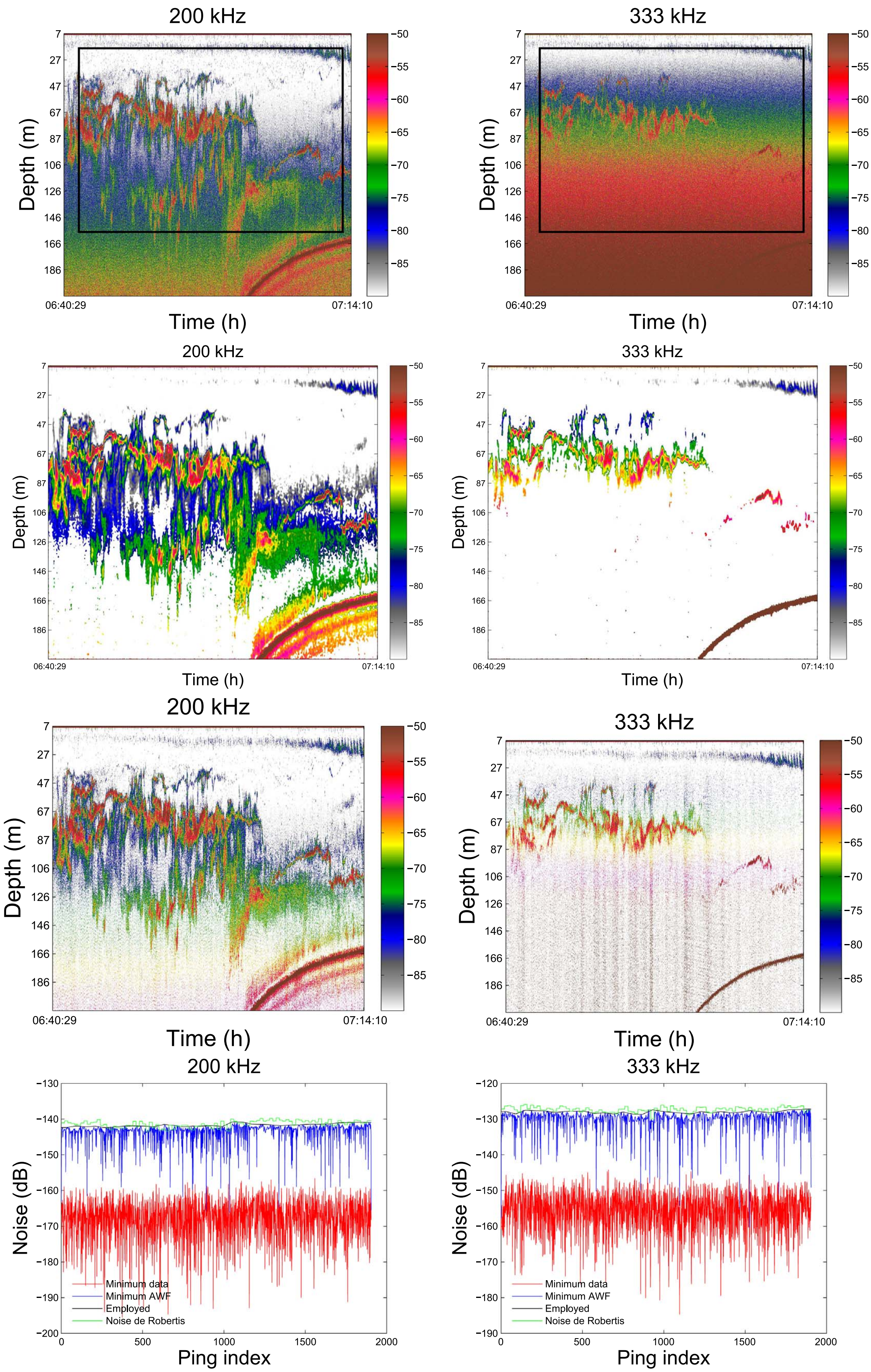

Fig. 2. Denoising of the 200 and 333 kHz, JUVENA 2013 survey data, showing: (first row) the original, (second row) the AWF denoising algorithm-processed, and (third row) the deRobertis and Higginbottom (2007) algorithm-processed echograms, and (forth row) the minimum *Sv* values before and after applying the AWF denoising ('minimum AWF') without TVG-amplification. The 'employed' level is the envelope of the minimum *Sv* values after smoothing. The noise level estimated by the deRobertis and Higginbottom (2007) method is also included. The square in the original echogram marks the area employed to calculate variables in Table 1.

contiguous sample; and (2) the percentage of biological pixels, that is, the pixels not included in the noise count and that were above the lower threshold (−90 dB). The nautical area scattering coefficient (NASC) values were calculated within the square, before and after denoising. The percentage of not thresholded pixels is given as ‘Data retained’.

2.3. Noise simulation

To see the influence of different noise types on echograms and the new algorithm performance, four noise cases are simulated (gaussian, speckle, ‘salt and pepper’ and impulse noise (Gonzalez and Woods, 2008)) and added to the 38 kHz echogram. Gaussian noise or white noise is an additive (independent of signal intensity) uncorrelated noise naturally present in images that is captured by instruments and adds variance to the signal. Speckle noise is a multiplicative (dependent of signal intensity) and locally correlated noise. In fisheries and plankton acoustics, speckle noise comes from the coherent nature of the scattering phenomenon: interferences due to multi-path reverberation of the sea floor (Anderson et al., 2007) or coherent summation of echoes coming from different targets. The latest depends on number of targets, frequency, pulse duration and pulse tapering (Gorska and Chu, 2005). Salt and pepper is a randomly distributed high intensity noise that can be the result of transmission or digital conversion errors and leaves high values in areas of low values and the contrary. Finally impulse noise refers to noise that has a particular direction and is often the result of interferences coming from other acoustic devices.

3. Results

Figs. 1 and 2 present the denoising results achieved with the AWF denoising algorithms (second row) and the deRobertis and Higginbottom (2007) algorithm (third row). The AWF denoising algorithm incremented the smoothing and maintained a clear visual separation of the structures in the echogram. The noise removal was similar with both techniques for the lower frequencies (Fig. 1). However, the AWF denoising algorithm produced smoother layers within the schools and their internal structures are clearer. The improvement is more noticeable in the 200 and 333 kHz echograms (Fig. 2), which were more affected by background noise amplified by TVG. Transducer ringing in the 18 kHz echogram (first 50 m) was not eliminated by either algorithm due to its homogeneous nature.

The final row of each figure shows the minimum *Sv* values per ping encountered for each frequency before (‘Minimum data’) and after applying the AWF filter (’Minimum AWF’), the employed noise value by the AWF denoising algorithm (’Employed’) and employed by the deRobertis and Higginbottom (2007) method (’noise de Robertis’) without TVG-amplification. The employed noise value corresponds to the envelope (maximum in a slide window) of the minimum *Sv* values after AWF smoothing. The noise profiles show an increase in noise at lower frequencies when close to the coastline due to bottom depth influence (Fig. 1 bottom). Noise levels calculated by the AWF denoising algorithm and the deRobertis and Higginbottom (2007) method are very similar, but the latter presents a more erratic path and the resulted cleaned image is better denoised with the former. The AWF denoising algorithm incremented the signal minimum level by ~20 dB. This value reflects the reduction in variability on the left side of the *Sv* distribution.

Table 1 includes the total echogram noise (‘Total noise’), and the selected region noise (‘% noise’) and biological percentages (‘% biol’). Noise was reduced in all cases using the AWF denoising

Table 1
Measurements of total noise (for the whole echogram), and percentage of biological pixels (% biol) and noise (% noise) in the region of interest (selected in the original echograms marked with a square), using the two methods described in this study. ‘Data retained’ gives the percentage of number of samples left with respect to the total number of samples in the echogram. The last column includes the nautical area scattering coefficient (NASC) calculated within the selected square. * These values indicate cases where the dedeRobertis and Higginbottom (2007) method presents more noise but the difference between the noise and the mean echogram values is lower than 10 dB, giving higher % biol and/or ‘Data retained’ values.

Method	Frequency (kHz)	Total Noise	%noise (domain)	%biol (domain)	Data retained (%)	NASC $\left(m^2/nmi^2\right)$
Original	18	2.4	12.7	75.0	80	314
Original	38	2.1	9.9	44.2	48	190
Original	200	3.7	26.0	51.5	74	1291
Original	333	4.8	37.5	60.7	89	9232
AWF	18	0.2	1.5	76.7	68	191
AWF	38	0.2	0.0	50.6	45	75
AWF	200	0.2	1.7	58.7	44	665
AWF	333	0.1	0.4	10.1	8.8	241
deRobertis	18	1.3	6.4	66.7	63	249
deRobertis	38	1.3	5.4	44.3	42	142
deRobertis	200	1.7	11.3	41.5	36	1070
deRobertis	333	1.8	10.0	*11.7	*14	1807

algorithm. The percentage of biological pixels was generally higher with the new method. However, in cases with high background noise amplified by TVG (marked with an asterisk), the noisy pixels were surrounded by other noise pixels with differences lower than 10 dB and were thus incorrectly selected as biological. Table 1 also reflects the percentages of pixels retained after denoising and nautical area scattering coefficient (NASC) values before and after denoising. As with %biol, only in cases of remaining TVG-amplified noise does the deRobertis and Higginbottom (2007) method keeps more data. NASC values are reduced due to noise removal. Mean SNR differences between both denoising methods calculated for each frequency showed slightly better values for the 18, 38 and 70 kHz echograms with the AWF denoising algorithm (≃1.5). The increase was more noticeable for high frequencies, with 2, 3 and 4 as the average increase in SNR for 120, 200 and 333 kHz respectively. For the latest case, 75% of the pixels presented higher SNR with the AWF denoising method.

Further results are shown for the 333 kHz frequency echogram in Fig. 3. The top figures show the logarithm of the local variance before (left) and after (right) the AWF denoising algorithm. The algorithm localises areas of higher variance and maintain those pixels practically unchanged, while smoothing out areas of low variance. The final variance echogram (top right) shows mainly the limits of schools and the bottom depth. The second row of figures presents the Sv vs depth plots of the first and last ten pings in the echogram before (left) and after (right) the AWF algorithm. The main ping pattern is kept while reducing inter-ping variability.

Fig. 4 shows the results of adding different noise types to the echogram into the estimated noise. The minimum *Sv* values before applying the AWF smoothing (‘minimum data’) show that with gaussian and speckle noise (top right and bottom left respectively) the tendency is maintained, although the Sv level is decreased. With Salt and pepper noise (bottom right), the minimum values are equivalent for all pings. In all cases, the AWF smoothing increments the minimum Sv level (‘minimum AWF’), finding a common envelope, although the variability is higher in the last case (Salt and pepper), due to the higher discrepancy of the starting level. In this latter case, applying smoothing a few more times would reach the same variability in the minimum Sv values

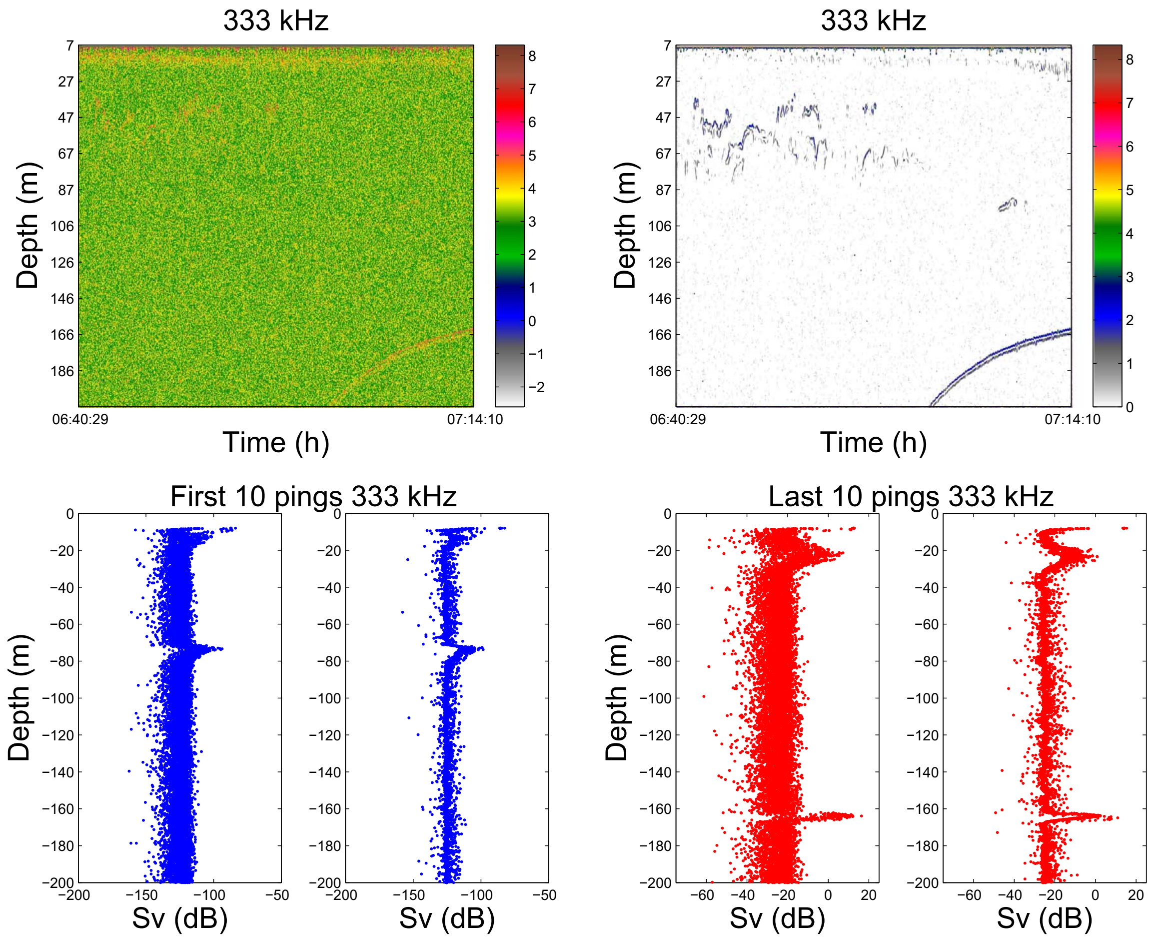

Fig. 3. Top row: logarithm of the local variances before and after applying AWF. Bottom row: 10 first and last pings of the 333 kHz echogram before (left) and after (right) applying AWF.

('minimum AWF'). Data retained is higher for these simulated examples, with 88%, 84% and 95% of samples kept for gaussian, speckle and salt and pepper noise respectively. As the real noise level has not been reached, more samples are kept. This is particularly noticeable in the right part of the echogram, on the coastal area, where the noise is near -135 dB for the original echogram, but nearer -140 dB for the salt and pepper noise case.

Finally in Fig. 5, a non-successful case is shown. A typical impulse noise coming from a different acoustic device is simulated, with contiguous samples of the same ping affected by noise. The top right figure shows the mask with the location of the column noise introduced on the 38 kHz echogram (top left). In this case, the second step of the algorithm, i.e. selecting the envelope of the minimum Sv values, would no be affected, as noise affects top *Sv* values. However, smoothing based on local variance is heavily affected as the local variance (bottom left) select these noisy samples as high local variance zones (i.e. as edges), keeping them unmodified (bottom right).

4. Discussion

This study has presented a denoising algorithm that improves the echogram data quality by applying a variance-dependent smoothing, reducing data variability. Cleaning was performed using a filter that adapts the smoothing to the local noise; higher variances at the edges resulted in less smoothing, maintaining their contrast, while the lower variances inside layers resulted in greater smoothing. This variance-dependent smoothing maintains the echogram structure, but reduces variability inside the echotraces preserving edge information. After improving data quality, the noise level is estimated as the envelope of the minimum Sv values. The denoising performance is more noticeable for higher frequencies where most of the noise is removed, while keeping more biological pixels in the echogram. Echograms of local variances prove that the AWF smoothing stops blurring at the edges, keeping better defined schools. deRobertis and Higginbottom (2007) suggested a noise-removal technique without smoothing, which requires a previous averaging technique. A gaussian filter using the smallest possible window (3×3 pixels) was applied in order to mix species as little as possible. Applying smoothing over a 5×5 window before the deRobertis and Higginbottom (2007) algorithm led to some blurring at the edges (results not included). The AWF denoising algorithm, on the other hand, applied smoothing based on variance and by applying it several times, the window size was not incremented each time, as the algorithm stopped smoothing when it reached an edge - that is, a high variance. Therefore, the window size is not incremented gradually.

Noise levels found by both methods are similar but, while the deRobertis and Higginbottom (2007) method subtract them from the data (needing later to threshold samples with SNR below zero), the AWF denoising algorithm threshold data with values below the noise level for the corresponding ping, as those samples are supposed to be corrupted by noise. The similarity in noise levels is due to the smoothing process that both apply to calculate it, but it is more effective with the AWF denoising algorithm as it uses local variance to prevent edges from being smoothed out, while the deRobertis and Higginbottom (2007) method smooths in

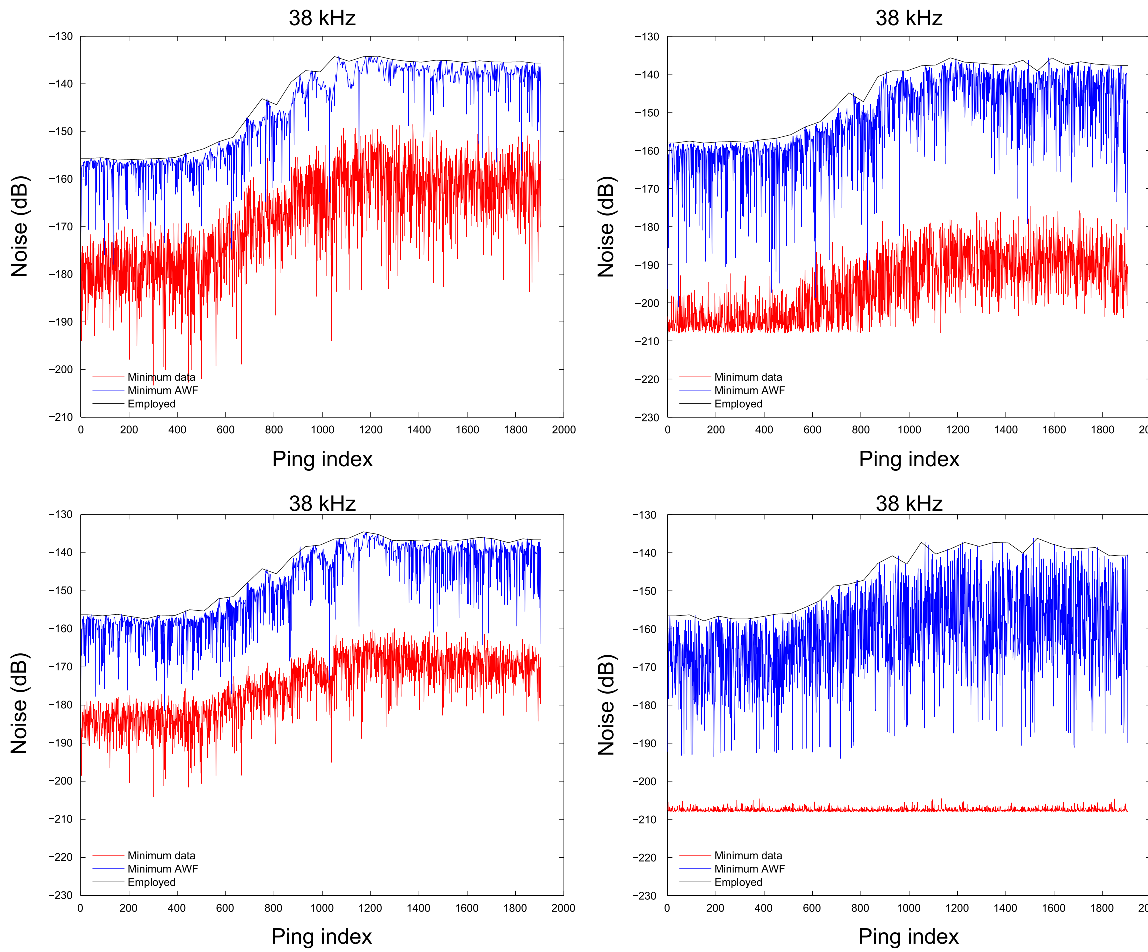

Fig. 4. Noise plots of the echograms: original (top left), affected by gaussian noise (top right), affected by speckle noise (bottom left) and affected by salt and pepper noise (bottom right).

pre-designed bins of M by N pixels, and only uses the averaging for noise estimation. The AWF denoising algorithm uses that information to reduce variance in the echogram, previous to noise estimation. deRobertis and Higginbottom (2007) proved that the found noise level is equivalent to the noise detected in passive mode, if the echogram includes samples corrupted by noise, i.e. if sufficient depth or samples below bottom depth are included. This is particularly relevant for the lower frequencies usually employed in fisheries and plankton acoustics.

This method is efficient in the presence of noise lasting for a sufficient number of pings (not impulse or transient noise of just a few pings), and with gaussian, speckle or salt and pepper noise. If impulse noise from an unsynchronised acoustic device is present, some preprocessing is needed to remove it. The denoising algorithms in Anderson et al. (2005) and Ryan et al. (2015) may be useful for this task. Although speckle noise due to coherent summation is negligible for echo integration (Gorska and Chu, 2005), it adds variability to the signal (Lavery et al., 2002) and can affect edges, shapes and intensity values of the echotraces. All these noises can be critical when comparing theoretical scattering models with multi-frequency observations for species identification and size estimation, or when studying echotraces' physical characteristics (shape, perimeter, height etc.). The increment in SNR with this new method permits to study low scatterers at deeper depth on high frequencies and a higher number of noise-free biological pixels are kept. This is particularly relevant for biomass estimation with higher frequencies or multi-frequency studies.

The AWF denoising algorithm presented in this study was proven successful with data from different vessels and noise conditions. I consider that it is particularly relevant to have adaptive noise-removal techniques for new vessels, where electrical machinery is incremented and presents varying frequencies that may increment or lower the noise in the echogram suddenly. No lower threshold was applied during processing, one was only used for the final visualisation. Thus, the algorithm is useful to clean data independently of the biological target to be studied and its Target Strength (TS). The AWF denoising algorithm can be used in cases of different background noise giving similar data quality and maximum SNR possible, which is fundamental to ensure accurate, repeatable and robust results.

5. Conclusion

I have presented a technique that firstly reduces data variability, homogenising echotraces but maintaining clear edges, and then removes noise of different typologies. The method automatically calculates the degree of smoothing necessary from the data variance, in an effort to smooth as much as possible, without averaging data from multiple species. After incrementing data quality, the denoising step removes noise corrupted data, outperforming previous techniques in high frequencies.

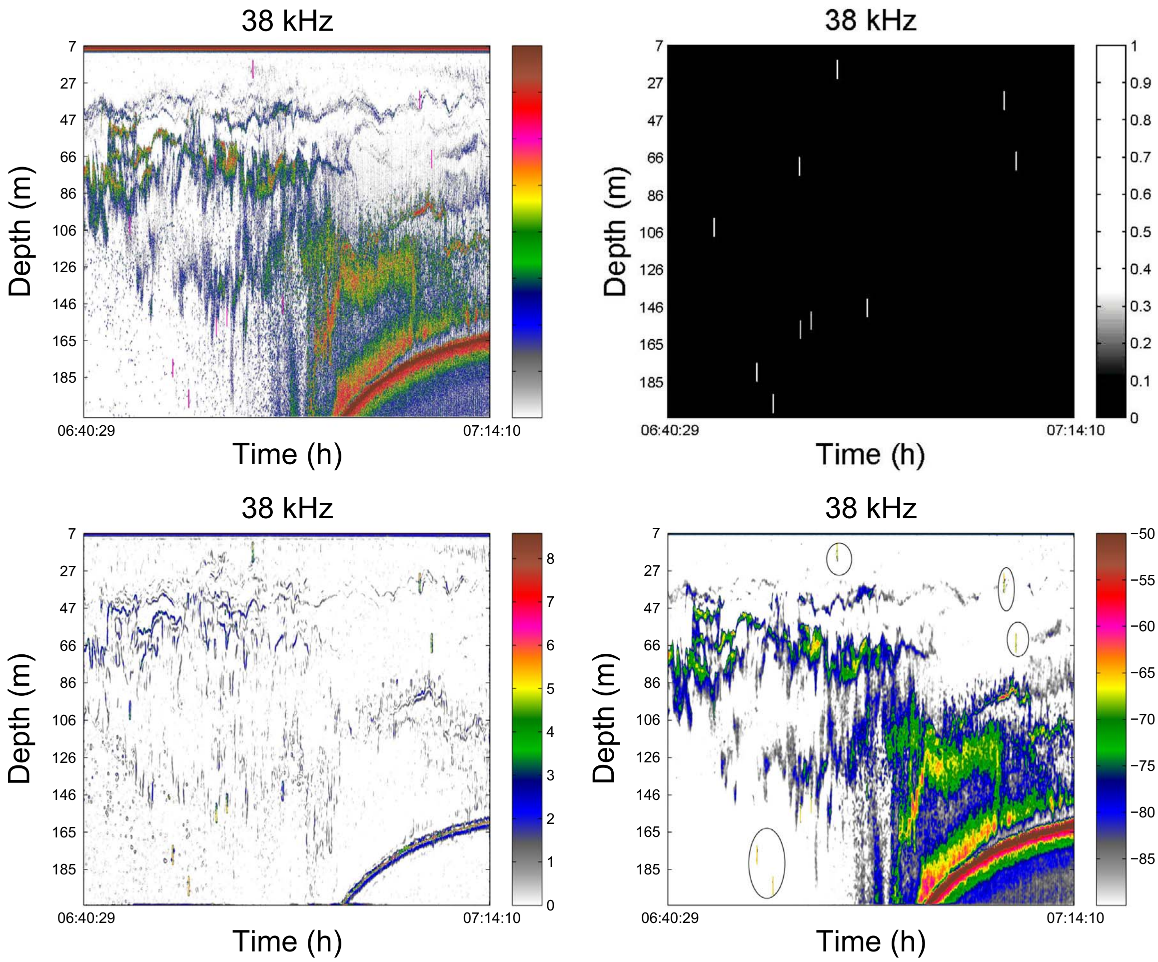

Fig. 5. Impulse noise example: the top figures show the noisy echogram on the left and the mask showing the location of the noise on the right. The bottom left figure shows the local variance after applying the AWF algorithm. The bottom right figure shows the resulting cleaned echogram with ellipses enclosing some remaining noises.

Acknowledgements

I thank the projects ‘Migrants and Active Flux In the Atlantic Ocean’ (MAFIA; CTM2012-39587-C04-03) and ‘The planktonic food-web in the Cantabrian Sea: Structure and biogenic CArbon PAthways’ (SCAPA; CTM2013-45089-R) for the support received. Thanks also to Alex de Robertis and the anonymous reviewers for some useful comments on the manuscript.

References

Abe, C., Shimamura, T., 2012. Iterative edge-preserving adaptive wiener filter for image denoising. Int. J. Comput. Electr. Eng. 4 (4), 503–506.
Anderson, C., Brierley, A., Armstrong, F., 2005. Spatio-temporal variability in the distribution of epi-and meso-pelagic acoustic backscatter in the Irminger sea, north Atlantic, with implications for predation on Calanus finmarchicus. Mar. Biol. 146 (6), 1177–1188.
Anderson, J.T., Holliday, V., Kloser, R., Reid, D., Simard, Y., 2007. Acoustic seabed classification of marine physical and biological landscapes. ICES Cooperative Research Report 2007. No 286, 198 pp.
Birdal, T., 2016. ⟨http://www.mathworks.com/matlabcentral/fileexchange/36941-fast-noise-estimation-in-images/content/estimate_noise.m⟩Matlab file exchange. Last accessed 02/05/2016.
Demer, D.A., Berger, L., Bernasconi, M., Bethke, E., Boswell, K., Chu, D., Domokos, R. et al., 2015. Calibration of acoustic instruments. Tech. rep., ICES Coop. Res. Rep. No. 326.
deRobertis, A., Higginbottom, I., 2007. A post-processing technique to estimate the signal-to-noise ratio and remove echosounder background noise. ICES J. Mar. Sci. 64, 1282–1291.
Gonzalez, R.C., Woods, R.E., 2008. Digital Image Processing. Prentice Hall.
Gorska, N., Chu, D., 2005. On the echo interference in sound backscattering by densely aggregated targets. ICES J. Mar. Sci. 62 (4), 771–778.
Immerkr, J., 1996. Fast noise variance estimation. Comput. Vis. Image Underst. 64 (2), 300–302.
Korneliussen, R.J., 2000. Measurement and removal of echo integration noise. ICES J. Mar. Sci.: J. du Cons. 57, 1204–1217.
Korneliussen, R.J., Ona, E., 2003. Synthetic echograms generated from the relative frequency response. ICES J. Mar. Sci. 60, 636–640.
Lavery, A.C., Stanton, T.K., Wiebe, P.H., 2002. Variability in High Frequency Acoustic Backscattering in the Water Column. In: Pace, N.G., Jensen, F.B. (Eds.), Impact of Littoral Environmental Variability of Acoustic Predictions and Sonar Performance. Kluwer Academic Publishers, pp. 63–70.
Lim, J.S., 1990. Two-Dimensional Signal and Image Processing. Prentice Hall,.
Nunnallee, E.P., 1990. An alternative to thresholding during echo-integration data collection. Rapp. P. -V. Réun. Cons. Int. Explor. Mer. 189, 92–94.
Peña, M., Olivar, M., Balbin, R., López-Jurado, J.L., Iglesias, M., Miquel, J., 2014. Acoustic detection of mesopelagic fishes in scattering layers of the Balearic sea (western Mediterranean). Can. J. Fish. Aquat. Sci. 71 (8), 1186–1197.
Ryan, T.E., Downie, R.A., Kloser, R.J., Keith, G., 2015. Reducing bias due to noise and attenuation in open-ocean echo integration data. ICES J. Mar. Sci. 72 (8), 2482–2493.
Watkins, J.L., Brierley, A.S., 1996. A post-processing technique to remove background noise from echo integration data. ICES J. Mar. Sci. 53, 339–344.